rent studies provide a conceptual framework for developing approaches to regulate T cell function through CTLA-4.

References and Notes

1. J. A. Bluestone, *J. Immunol.* **158**, 1989 (1997); A. I. Sperling and J. A. Bluestone, *Immunol. Rev.* **153**, 155 (1996).
2. C. R. Calvo, D. Amsen, A. M. Kruisbeek, *J. Exp. Med.* **186**, 1645 (1997), P. S. Linsley *et al.*, *Immunity* **4**, 535 (1996); M. Griffin and J. A. Bluestone, unpublished observations.
3. W. Zhang *et al.*, *Cell* **92**, 83 (1998).
4. K.-M. Lee *et al.*, unpublished observation.
5. A. M. Weissman, L. E. Samelson, R. D. Klausner, *Nature* **324**, 480 (1986); M. Baniyash *et al.*, *J. Biol. Chem.* **263**,18225 (1988).
6. P. W. Wallace *et al.*, *Transplantation* **58**, 602 (1994).
7. F. Letourneur and R. Klausner, *Science* **255**, 79 (1992).
8. J. D. Bradshaw *et al.*, *Biochemistry* **36**, 15975 (1997); E. Chuang *et al.*, *J. Immunol.*, in press.
9. L. E. Marengere *et al.*, *Science* **272**, 1170 (1996).
10. P. J. Blair *et al.*, *J. Immunol.* **160**, 12 (1998).
11. A. Kupfer and S. J. Singer, *Proc. Natl. Acad. Sci. U.S.A.* **85**, 8216 (1988); C. B. Thompson and J. P. Allison, *Immunity* **7**, 445 (1997).
12. E. Chuang *et al.*, *J. Immunol.* **159**, 144 (1997); Y. Zhang and J. P. Allison, *Proc. Natl. Acad. Sci. U.S.A.* **94**, 9273 (1997).
13. G. Feng *et al.*, *Science* **259**, 1607 (1993); W. Vogel *et al.*, *ibid.*, p. 1611; T. Tauchi *et al.*, *J. Biol. Chem.* **269**, 15381 (1994).
14. E. N. Kersh, A. S. Shaw, P. M. Allen *Science* **281**, 572 (1998).
15. T. L. Walunas *et al.*, *Immunity* **1**, 405 (1994).
16. O. Leo *et al.*, *Proc. Natl. Acad. Sci. U.S.A.* **84**, 1374 (1987).
17. R. Abe *et al.*, *J. Immunol.* **154**, 985 (1995).
18. B. A. Houlden, R. Q. Cron, J. E. Coligan, J. A. Bluestone, *ibid.* **141**, 3753 (1988).
19. T cells from BALB/c lymph nodes were purified (*15*) and cultured for 60 hours in a dish coated with mAb to CD3 (anti-CD3) (145-2C11; 2 μg/ml) (*16*) and mAb to CD28 (anti-CD28) (PV-1; 2 μg/ml) (*17*). Cells were then washed three times to remove any residual antibodies present on the cell surface and rested at 37°C for additional 4 hours.
20. M. Griffin *et al.*, unpublished data.
21. Immunoprecipitations were performed with lysates prepared in LB [1% Nonidet P-40, 50 mM tris-HCl (pH 7.4), 150 mM NaCl, 20 mM EDTA (pH 8.0), 1 mM sodium vanadate, leupeptin (10 μg/ml), 10 μM aprotinin, 1 mM phenylsulfonylsulfoxide]. Lysates were precleared twice with protein A beads and once with protein A beads coated with a mAb from a control hamster (UC3-10A6) (*18*) before precipitating antibodies were added. Immunoprecipitation was performed overnight at 4°C. Immune complexes were washed five times with LB and subjected to SDS-PAGE.
22. M. M. Rozdzial, R. T. Kubo, S. L. Turner, T. H. Finkel *J. Immunol.* **153**, 1563 (1994).
23. BALB/c whole lymph node and spleen T cells were activated with mAb 145-2C11 (1 μg/ml) plus mAb PV-1 (1 μg/ml) for 60 hours. Cells were washed and rested as described (*19*). Viable cells were enriched by passage over Ficoll/Hypaque. Over 90% of viable cells were $CD3^+$ by fluorescence-activated cell sorter analysis.
24. D. G. Orloff *et al.*, *J. Biol. Chem.* **264**, 14812 (1989).
25. The CTLA-4 tyrosine mutant (Y201F/Y218F) was generated by site-directed mutagenesis (Chameleon site-directed mutagenesis kit, Stratagene) and the presence of mutations was verified by DNA sequencing. A cDNA sequence incorporating the coding region of murine TCRζ was generated by reverse transcription and polymerase chain reaction from RNA extracted from activated murine T cells and cloned into the mammalian expression vector pCDNA3.1(+).
26. A. C. Carrera *et al.*, *Proc. Natl. Acad. Sci. U.S.A.* **90**, 442 (1993).
27. T. Yin, R. Shen, G. S. Feng, Y. C. Yang, *J. Biol. Chem.* **272**, 1032 (1997).

28. Supported by the National Institutes of Health (PHS PO1 AI35294-6). Additional support was provided by a Howard Hughes Medical Institute Medical Student Research Training Fellowship (D.K.H.) and a Mayo Foundation Scholarship (M.G.). We thank G. Feng for the reagents; A. Sharpe for CTLA-4 knockout mice; N. Patel and C. Long for technical assistance; S. Thomas, M. Fonstein, and W. Buikema for services provided at the Cancer Research Center (CRC) DNA Sequencing Facility; and M. Clark for critical reading of the manuscript.

10 August 1998; accepted 10 November 1998

A Receptor/Cytoskeletal Movement Triggered by Costimulation During T Cell Activation

Christoph Wülfing and Mark M. Davis*

During T cell activation, the engagement of costimulatory molecules is often crucial to the development of an effective immune response, but the mechanism by which this is achieved is not known. Here, it is shown that beads attached to the surface of a T cell translocate toward the interface shortly after the start of T cell activation. This movement appears to depend on myosin motor proteins and requires the engagement of the major costimulatory receptor pairs, B7-CD28 and ICAM-1–LFA-1. This suggests that the engagement of costimulatory receptors triggers an active accumulation of molecules at the interface of the T cell and the antigen-presenting cell, which then increases the overall amplitude and duration of T cell signaling.

The central event in T cell activation is the interaction of the T cell receptor (TCR) with the antigenic peptide presented by the major histocompatibility complex (MHC) of the antigen-presenting cell (APC). However, because the number of agonist peptide–MHC complexes can be very low, in the range of 10 to 100 per APC (*1*), and because the TCR is continuously modulated from the T cell surface (*2*), sustained T cell activation is likely to require signal amplification (*3, 4*). An important component of this amplification is thought to be provided by costimulatory molecules on the T cell, although the mechanism by which they accomplish it is unclear (*5*). The most important of the costimulatory receptors on T cells and their ligand on APCs are CD28-B7 (*6*) and LFA-1–ICAM-1 (*7*). Many different receptor couples, including TCR–peptide-MHC and LFA-1–ICAM-1, accumulate at the T cell–APC interface (*8, 9*). This accumulation has been assumed to be a passive, diffusion-limited cocapping mechanism (*10*). Here, we describe an active, cytoskeletal mechanism that appears to drive receptor accumulation at the T cell–APC interface. This mechanism requires the APC to express B7 and ICAM-1 and is independent of TCR signaling. We suggest that this mechanism is a central part of costimulation, as it would effectively amplify any TCR-mediated signals.

Howard Hughes Medical Institute and Department of Microbiology and Immunology, Stanford University School of Medicine, Stanford, CA 94305, USA.

*To whom correspondence should be addressed.

To study whether receptor accumulation at the T cell–APC interface could be actively driven by the T cell cytoskeleton, we monitored the general movement of the cortical actin cytoskeleton and linked receptors (*11*) using the classical technique of attaching large beads to the surfaces of antigen-specific T cells. We coated 4.5-μm beads with an antibody to the T cell surface antigen ICAM-1 (*12*). Cross-linking ICAM-1 by beads in this way is not expected to influence T cell function (*13*). As has been observed with fibroblasts (*11, 14*), we find that in migrating 5C.C7 transgenic T cells (*9, 15*) the beads translocate from the anterior to the posterior end of the cell (*16*). We then mixed bead-loaded 5C.C7 T cells with B cell lymphoma cells that express the appropriate MHC molecule ($I\text{-}E^k$) and have been pulsed with the moth cytochrome c peptide 88-103. After contact with the APC, the T cells rapidly become activated (*9, 17*) and the beads move from the posterior end of the T cell to the newly formed interface with the B cells (Fig. 1, movie 1) beginning 4 ± 1 min after the first rise in intracellular calcium (n = 13). This suggests that the T cell cortical actin cytoskeleton reorients toward the T cell–APC interface soon after the start of T cell activation. The ensuing cytoskeletal flow would allow receptors that are linked to the actin cytoskeleton to be transported to the newly formed T cell–APC interface.

To rule out ICAM-1–specific effects, we also attached beads to T cells in two other ways. First, we surface-biotinylated the 5C.C7 T cells with an amine-reactive form of biotin and used

2.8-μm streptavidin beads (*18*). Second, we exchanged a lipid that is biotinylated at its head into the cell surface of the T cells from liposomes (*19*) and used the same 2.8-μm streptavidin beads (*20*). In both cases, we found a behavior identical to that of the antibody-coated beads (Table 1). This confirms that the beads monitor the movement of the cortical actin cytoskeleton and not that of a specific receptor. We have also obtained identical results using monocytes and dendritic cells prepared directly ex vivo as APCs (*16*). The time to travel half a cell circumference is 6 ± 2 min (n = 14). Given that the diameter of our activated T cells is ~10 μm, this speed of ~3 μm/min is similar to that reported in comparable studies on migrating fibroblasts (1 to 5 μm/min) (*21*). This behavior is independent of the peptide concentration on the APC as long as enough peptide is presented to activate the T cell (*16*). Beads bound to the B cell do not move, consistent with the lack of involvement of the B cell actin cytoskeleton in the redistribution of specific receptors (*9, 22*).

To study the role of costimulatory receptor pairs in the regulation of the cytoskeletal movement, we added antibodies that block a number of accessory interactions to this system. We found that blocking ICAM-1 or B7-1 together with B7-2 abolishes bead movement while leaving undisturbed other aspects of T cell activation, such as the formation of a tight interface and the elevation of intracellular calcium (Table 1) (*16*). Antibodies to CD48 or VCAM had no effect (Table 1). To determine whether the interactions of ICAM-1 with LFA-1 or of B7 with CD28 are sufficient to trigger bead movement, we used transfected CHO cells as APCs. When transfected with I-E^k, the CHO cells were not able to induce bead movement (Table 1). When the CHO cells were transfected with I-E^k and either ICAM-1 or B7-2 gene constructs, we observed a partial restoration of the bead movement (Table 1). The best results were obtained by transfecting ICAM-1 and engaging CD28 on the T cell with an activating antibody, which allows bead movement to near B cell levels (Table 1). Preliminary experiments with CHO cells expressing all three molecules (I-E^k, ICAM-1, and B7-2) showed that 7 of 10 T-CHO couples examined moved beads toward the T cell–APC interface (*16*). These experiments show that the interactions of LFA-1–ICAM-1 and CD28-B7 are both necessary and sufficient to induce movement of the T cell cortical actin cytoskeleton toward the newly formed T cell–APC interface.

We have also characterized second messengers that are synergistically activated by the TCR and the accessory interactions that are

Table 1. Occurrence of different types of T cell bead movement (*39*) during the interaction of a 5C.C7 T cell with APCs loaded with an activating peptide. Unless mentioned, the APCs were CH27 B cell lymphomas. Bead movement was analyzed using three different types of beads (*12, 18, 20*); only two of these bead types (*12, 18*) were used for the rest of the experiments. Blocking antibodies and pharmacological agents were used under standard conditions. (*40*). The number of cells analyzed during wortmannin treatment was small because the majority of the T cells did not establish a polarized phenotype (*41*). When transfected CHO cells were used as APCs, we found that GFP fusion did not inhibit the function of its fusion partner (*9, 22*). In the last row, an activating antibody to CD28 was present during the interaction of the T cell and APC; n indicates the number of cells studied (*34*).

Type of beads/treatment/APC	Movement toward interface	Movement away from interface	No movement	n
Type of beads				
Anti-ICAM	74%	0%	26%	81
Streptavidin (surface biotin)	83%	7%	10%	29
Streptavidin (lipid biotin)	64%	5%	32%	22
Antibody blocking				
anti-ICAM	11%	5%	84%	37
anti-B7	8%	0%	92%	24
anti-VCAM	62%	0%	38%	21
anti-CD48	75%	0%	25%	20
Pharmacological agents				
Wortmannin	13%	0%	78%	8
Ni/BAPTA	23%	0%	77%	26
Transfected CHO cells as APCs				
CHO/I-E^k	4%	0%	96%	47
CHO/I-E^k/ICAM-1–GFP	27%	7%	67%	45
CHO/I-E^k/B7-2–GFP	34%	2%	64%	47
CHO/I-E^k/ICAM-1–GFP (anti-CD28)	59%	0%	41%	27

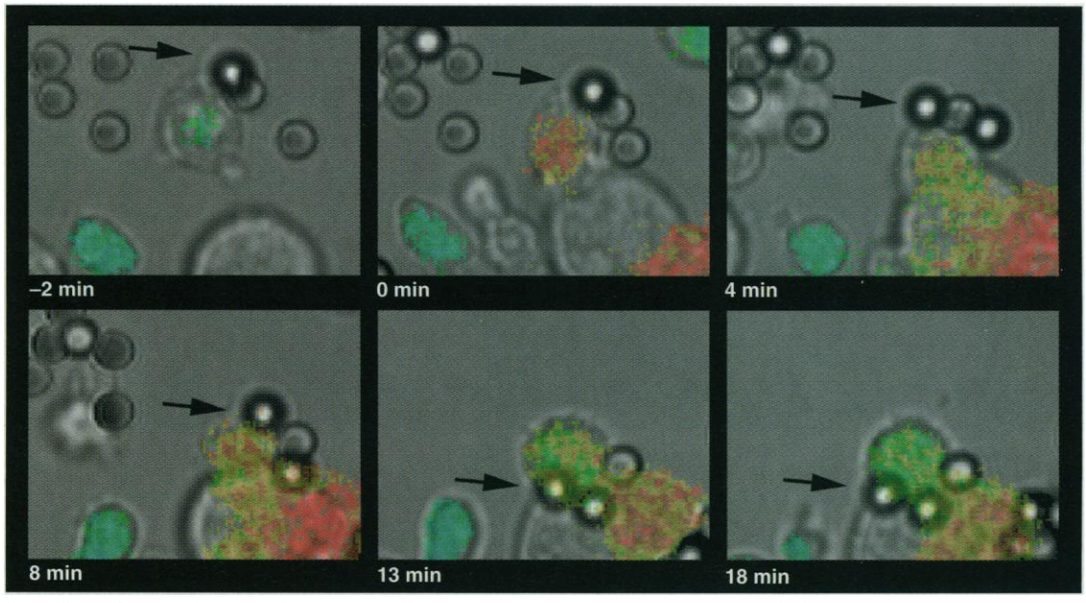

Fig. 1. Bead movement toward the interface. Single frames of a video microscopy experiment (*36*) of the interaction of 5C.C7 T cells, loaded with 4.5-μm anti–ICAM-1 (YN1) beads, with peptide-loaded CH27 B cell lymphoma cells (*35*) are shown. The CH27 cell is substantially larger than the T cells. The T cell intracellular calcium concentration is overlaid in a false color scale from blue (low concentration) to red (high concentration) to mark the onset of T cell activation, set to time 0:00 min. Although the beads, one of which is marked with an arrow, are bound to the posterior end of the central T cell before and at the time of its activation, they can be seen to move toward the T cell–B cell interface in subsequent frames. The still frames have been excerpted from movie 1 (*37*), which can be viewed at *Science* Online (www.sciencemag.org).

important for bead movement, namely the intracellular calcium concentration for ICAM-1–LFA-1 (*9, 23*) and the phosphatidylinositol 3-kinase (PI 3-kinase) for B7-CD28 (*24*). Blocking the rise in the intracellular calcium concentration with 1,2-bis(2-aminophenoxy)ethane-*N*,*N*,*N*′,*N*′-tetraacetic acid (BAPTA) and Ni^{2+} blocks bead movement (Table 1) while leaving the formation of a tight interface intact (*9*). Using the PI 3-kinase inhibitor wortmannin (*25*) at 100 nM leads to a distinct phenotype in that most T cells do not establish a polarized phenotype before activation. For the minority of T cells that display a polarized phenotype, bead movement is abolished. These results are consistent with both PI 3-kinase and intracellular calcium being necessary for bead movement.

The cortical actin cytoskeleton moves either by controlled assembly and disassembly of actin filaments or by sliding actin filaments past each other using myosin motor proteins (*11, 26*). In particular, myosin motor proteins are thought to be involved in actin cytoskeleton movement at the cell body (*21*). Previously, we and others have shown that blocking actin filament assembly in the T cell (but not B cell APCs) with cytochalasin D severely disrupts many aspects of T cell activation (*3, 9*). Inhibiting the myosin motors with butanedione monoxime (BDM) (*27*) gives a more specific phenotype in this system, as shown in Fig. 2 (movie 2) and Table 2. At high concentrations of BDM, the diameter of the T cell–B cell interface is reduced, the calcium signal is less sustained, the redistribution of ICAM-1 to the T cell–B cell interface is impaired, the redistribution of I-E^k is inhibited (*22*), and bead movement is partially blocked (Table 2). At low BDM concentrations (2 mM), the reduction in interface diameter and the impairment of bead movement remain (Table 2), suggesting that myosin motors are most involved in these two processes. Because BDM has also been reported to block T cell potassium uptake (*28*), we inhibited voltage-gated potassium channels specifically with noxius toxin (*29*) and found no inhibition of bead movement (Table 2). The small effect we see on early T cell activation is consistent with the moderate effects reported for specific potassium channel blockers on later activation events (*30*). We conclude that the receptor/cytoskeletal movement that we describe here is dependent on myosin motor proteins.

In vivo, costimulation is usually required for efficient T cell activation, probably because TCR signaling is limited by small numbers of agonist peptide–MHC complexes and continuous internalization of the TCR-CD3 complex. Previously, we have shown that the accumulation of MHC-peptide–TCR and accessory receptor couples at the T cell–APC interface after T cell activation can amplify the weak TCR signal efficiently (*9, 22*). Here, we have described an active movement of the cortical actin cytoskeleton toward the interface, involving myosin motor proteins, that would move all molecules linked to the actin cytoskeleton toward the T cell–APC interface. In support of this possibility, we find that the increase in concentration of LFA-1–ICAM-1 and other (TCR–peptide–I-E^k and CD2-CD48) receptor couples at the interface

Table 2. Effects of blocking myosin motor proteins. The analysis of T cell activation by peptide loaded CH27 cells in the presence of BDM or noxius toxin (NTX) is shown (*42*). Narrow interface form denotes activated T cells having a T cell–B cell interface diameter that is smaller than the diameter of the T cell (Fig. 2). Calcium signal back to baseline denotes activated T cells whose intracellular calcium concentration returns to preactivation levels during an observation period of at least 5 min. ICAM cluster formation denotes CH27 cells that show accumulation of ICAM-1–GFP at the T cell–B cell interface after T cell activation (*9*) (Fig. 2). Bead movement toward the interface (*39*) refers to activated T cells that show anti–ICAM-1 bead movement. In all cases, *n* denotes the number of cells analyzed (*43*).

Pharmacol. agent	Interface form		Calcium signal		ICAM clustering		Bead movement	
	Narrow	*n*	Back to baseline	*n*	Cluster formation	*n*	Toward interface	*n*
BDM (20 mM)	93%	55	68%	108	36%	33	19%	27
BDM (10 mM)	79%	58	45%	83	51%	35	27%	15
BDM (2 mM)	70%	46	23%	73	85%	32	25%	28
Buffer alone	14%	56	2%	102	90%	38	62%	21
NTX (100 nM)	23%	47	9%	76	85%	40	63%	27

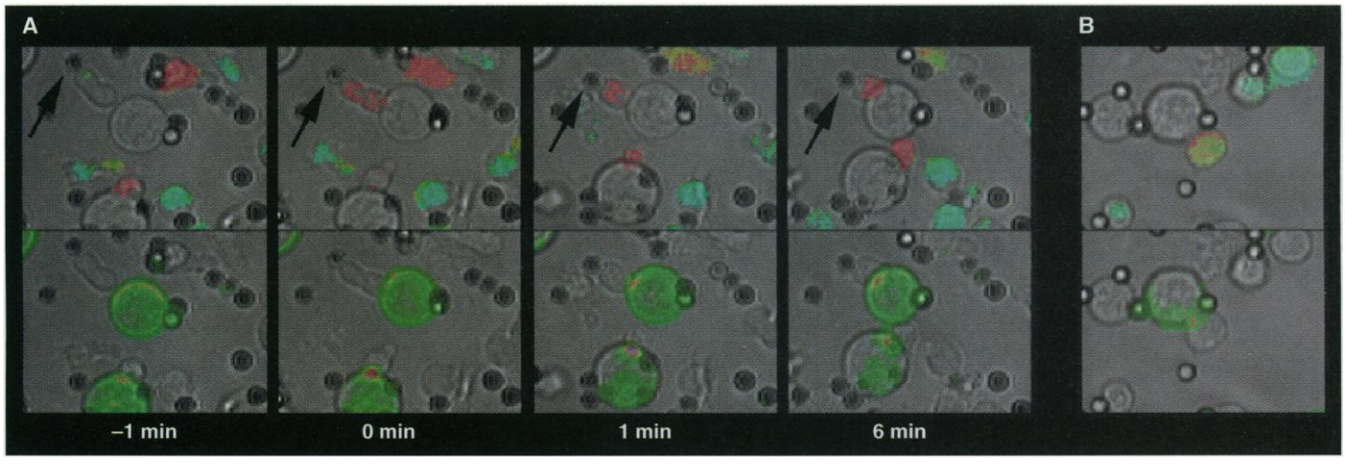

Fig. 2. T cell–APC interaction with blocked myosin motor proteins. (**A**) Single frames of a video microscopy experiment (*36*) of the interaction of 5C.C7 T cells, loaded with 4.5-μm anti–ICAM-1 (YN1) beads, with peptide-loaded, ICAM-1–GFP–transfected CH27 cells are shown. The bright-field image has been duplicated. In the top panels, the T cell intracellular calcium concentration is overlaid in a false color scale as in Fig. 1. In the bottom panels, the ICAM-1–GFP fluorescence is overlaid in a false color scale from green (low fluorescence) to blue (high fluorescence) to allow the simultaneous investigation of the additional cellular parameter. The accumulation of ICAM-1 at the T cell–APC interface in the absence of all pharmacological agents was described in (*9*); here, such an interaction is shown in the presence of 2 μM BDM. Although the calcium signal is elevated in a stable manner and ICAM-1–GFP accumulates at the interface, this interface is narrow (as most easily seen by the tightly concentrated ICAM-1–GFP accumulation), and a bead that is bound to an activating T cell, marked with an arrow, does not move. The still frames were excerpted from movie 2 (*38*), which can be viewed at *Science* Online (www.sciencemag.org). (**B**) An even narrower interface at 20 μM BDM, excerpted from a movie of a different experiment.

and the movement of the cortical cytoskeleton are regulated similarly. Both processes are sensitive to the myosin inhibitor BDM, to anti-B7, and to the choice of APC (*9, 22*) (Table 2). Furthermore, we have shown that this movement of the actin cytoskeleton is regulated by the two most important costimulatory receptor pairs, CD28-B7 and LFA-1–ICAM-1. We suggest that this active accumulation of receptor pairs and other cytoskeleton-linked molecules at the T cell–APC interface, and the signal amplification that would result from these increased receptor densities, could be the principal basis of the costimulatory effect. This is in contrast to models in which a costimulatory signal integrates with TCR signals in the nucleus to affect gene expression.

References and Notes

1. S. Demotz, H. M. Grey, A. Sette, *Science* **249**, 1028 (1990); C. V. Harding and E. R. Unanue, *Nature* **346**, 574 (1990); R. C. Brower *et al.*, *Mol. Immunol.* **31**, 1285 (1994); Y. Sykulev, M. Joo, I. Vturina, T. J. Tsomides, H. N. Eisen, *Immunity* **4**, 565 (1996); J. Delon, N. Bercovici, G. Raposo, R. Liblau, A. Trautmann, *J. Exp. Med.* **188**, 1473 (1998).
2. S. Valitutti, S. Müller, M. Cella, E. Padovan, A. Lanzavecchia, *Nature* **375**, 148 (1995); S. Valitutti, S. Müller, M. Salio, A. Lanzavecchia, *J. Exp. Med.* **185**, 1859 (1997).
3. S. Valitutti, M. Dessing, K. Aktories, H. Gallati, A. Lanzavecchia, *J. Exp. Med.* **181**, 577 (1995).
4. G. Iezzi, K. Karjalainen, A. Lanzavecchia, *Immunity* **8**, 89 (1998); L. J. Holsinger *et al.*, *Curr. Biol.* **8**, 563 (1998).
5. C. G. Sagerstrom, E. M. Kerr, J. P. Allison, M. M. Davis, *Proc. Natl. Acad. Sci. U.S.A.* **90**, 8987 (1993); M. Croft and C. Dubey, *Crit. Rev. Immunol.* **17**, 89 (1997); S. L. Swain *et al.*, *Immunol. Rev.* **150**, 143 (1996); M. F. Bachmann *et al.*, *Immunity* **7**, 549 (1997).
6. C. A. Chambers and J. P. Allison, *Curr. Opin. Immunol.* **9**, 396 (1997); P. J. Blair *et al.*, *Biochem. Soc. Trans.* **25**, 651 (1997); A. I. Sperling and J. A. Bluestone, *Immunol. Rev.* **153**, 155 (1996).
7. M. L. Dustin and T. A. Springer, *Nature* **341**, 619 (1989); Y. van Kooyk and C. G. Figdor, *Biochem. Soc. Trans.* **25**, 515 (1997); M. Stewart and N. Hogg, *J. Cell. Biochem.* **61**, 554 (1996).
8. A. Kupfer and S. J. Singer, *Annu. Rev. Immunol.* **7**, 309 (1989); C. R. Monks, B. A. Freiberg, H. Kupfer, N. Sciaky, A. Kupfer, *Nature* **395**, 82 (1998).
9. C. Wülfing, M. D. Sjaastad, M. M. Davis, *Proc. Natl. Acad. Sci. U.S.A.* **95**, 6302 (1998).
10. S. J. Singer, *Science* **255**, 1671 (1992).
11. As reviewed by M. D. Sheets, R. Simson, K. Jacobson, *Curr. Opin. Cell Biol.* **7**, 707 (1995); M. S. Bretscher, *Cell* **87**, 601 (1996).
12. Dynabeads (M450; Dynal) coated with sheep antisera to rat immunoglobulin were coated with YN1 (*31*) at 4°C at 160 μg per 10^7 beads. For microscopy, beads were used at a 2:1 ratio over T cells. Half of the beads were preincubated with the T cells at 4°C; the other half were added to the T cells on the microscopy stage.
13. H. Xu *et al.*, *J. Exp. Med.* **180**, 95 (1994); J. E. Sligh Jr. *et al.*, *Proc. Natl. Acad. Sci. U.S.A.* **90**, 8529 (1993).
14. B. F. Holifield, A. Ishihara, K. Jacobson, *J. Cell Biol.* **111**, 2499 (1990); D. A. Lauffenberger and A. F. Horwitz, *Cell* **84**, 359 (1996).
15. R. A. Seder, W. E. Paul, M. M. Davis, B. Fazekas de St. Groth, *J. Exp. Med.* **176**, 1091 (1992).
16. C. Wülfing and M. M. Davis, data not shown.
17. P. A. Negulescu, T. B. Krasieva, A. Khan, H. H. Kerschbaum, M. D. Cahalan, *Immunity* **4**, 421 (1996).
18. T cells were surface-biotinylated after loading them with Fura-2 by incubating 10^6 T cells for 30 min at 4°C in Ringer's buffer [10 mM Hepes (pH 7.4), 154 mM NaCl, 7.2 mM KCl, and 1.8 mM $CaCl_2$] with sulfo-NHS-biotin (200 μg/ml; Pierce, Rockford, IL). After washing the cells into 10% fetal bovine serum in phosphate-buffered saline (PBS) with 1 mM $CaCl_2$ and 0.5 mM $MgCl_2$ at 4°C, they were used within 2 hours. Streptavidin-coated Dynabeads (M280; Dynal) were used as described for the YN1-coated beads.
19. A. E. Ting and R. E. Pagano, *J. Biol. Chem.* **265**, 5337 (1990).
20. Biotinylated lipids were incorporated into the T cell membrane from liposomes consisting of 85% egg phosphatidylcholine (Sigma), 10% *N*-([6-(biotinoyl)amino]-hexanoyl)1,2-dihexadecanoyl-*sn*-glycero-3-phosphoethanolamine (Molecular Probes), and 5% *N*-(7-nitrobenz-2-oxa-1,3-diazol-4-yl)-1,2-dihexadecanoyl-*sn*-glycero-3-phosphoethanolamine (Molecular Probes), prepared as described (*32*). The biotinylated lipids were incorporated into the T cell membrane by incubating 10^6 T cells for 1 hour with the liposomes at a lipid concentration of 0.1 mg/ml in PBS with 1 mM $CaCl_2$ and 0.5 mM $MgCl_2$.
21. J. P. Heath and B. F. Holifield, *Symp. Soc. Exp. Biol.* **47**, 35 (1993).
22. C. Wülfing and M. M. Davis, unpublished data.
23. P. Kuhlman, V. T. Moy, B. A. Lollo, A. A. Brian, *J. Immunol.* **146**, 1773 (1991); S. B. Kanner, L. S. Grosmaire, J. A. Ledbetter, N. K. Damle, *Proc. Natl. Acad. Sci. U.S.A.* **90**, 7099 (1993).
24. S. G. Ward, C. H. June, D. Olive, *Immunol. Today* **17**, 187 (1996); A. Toker and L. C. Cantley, *Nature* **387**, 673 (1997).
25. H. Yano *et al.*, *J. Biol. Chem.* **268**, 25846 (1993); R. Woscholski, T. Kodaki, M. McKinnon, M. D. Waterfield, P. J. Parker, *FEBS Lett.* **342**, 109 (1994).
26. As reviewed by M. F. Carlier and D. Pantaloni, *J. Mol. Biol.* **269**, 459 (1997); S. K. Maciver, *Bioessays* **18**, 179 (1996).
27. L. P. Cramer and T. J. Mitchison, *J. Cell Biol.* **131**, 179 (1995).
28. L. C. Schlichter, P. A. Pahapill, I. Chung, *J. Pharmacol. Exp. Ther.* **261**, 438 (1992).
29. S. Grissmer *et al.*, *Mol. Pharmacol.* **45**, 1227 (1994).
30. J. A. Verheugen, F. Le Deist, V. Devignot, H. Korn, *Cell Calcium* **21**, 1 (1997) and references therein.
31. F. Takei, *J. Immunol.* **134**, 1403 (1985).
32. J. T. Groves, C. Wülfing, S. G. Boxer, *Biophys. J.* **71**, 2716 (1996).
33. K. Miyake *et al.*, *J. Cell Biol.* **114**, 557 (1991); K. Miyake, I. L. Weissman, J. S. Greenberger, P. W. Kincade, *J. Exp. Med.* **173**, 599 (1991).
34. The results are derived from a composite analysis of at least seven experiments (11 on average) performed on at least two different days (four on average) for each condition. We show a composite analysis because on average only three or four cells per experiment could be analyzed. To ensure consistency within the data set, at least one positive control experiment was included during each day of experiments.
35. The CH27 cells used in this particular experiment were ICAM-1–GFP transfected. ICAM-1–GFP transfection of the CH27 cells has no effect on the bead movement (*16*). The ICAM-1–GFP fluorescence is not shown.
36. Peptide loading of APCs using 10 μM moth cytochrome c peptide 82-103, Fura-2 loading of T cells, and microscopy (using the Zeiss/Attofluor system) were performed as in (*9*).
37. Movie 1: Bead movement toward the interface. The interaction of 5C.C7 T cells, loaded with 4.5-μm anti–ICAM-1 (YN1) beads, with peptide-loaded CH27 B cell lymphoma cells (*35*) is shown. The CH27 cell is substantially larger than the T cells. Although the beads are bound to the posterior end of the top T cell before and at the time of its activation, they can be seen to move toward the T cell–B cell interface in subsequent frames. The T cell intracellular calcium concentration is overlaid in a false color scale. Two closely related calcium-sensitive dyes that differ in their calcium dissociation constant, Fura-PE in movie 1 and Fura-2 in movie 2, have been used. Therefore, blue indicates low calcium concentration in both movies, whereas high calcium concentration is encoded in yellow in movie 1 and in red in movie 2. For reasons of simplicity, in Fig. 1 the calcium color scale has been changed from the original one of movie 1 to match that of movie 2/Fig. 2. The movie compresses 20 min of experiment into 1 min of movie.
38. Movie 2: T cell–APC interaction with blocked myosin motor proteins. The interaction of 5C.C7 T cells, loaded with 4.5-μm anti–ICAM-1 (YN1) beads, with peptide-loaded, ICAM-1–GFP–transfected CH27 B cell lymphoma in the presence of 2 mM BDM is shown. A bright-field series of images has been duplicated and is overlaid with false-color encoded fluorescence information. The top panel is overlaid with a false-color representation of the intracellular calcium concentration of the T cell, ranging from blue (low concentration) to red (high concentration). In the bottom panel, the ICAM-1–GFP fluorescence of the B cell lymphoma is overlaid in a false color scale from green (low fluorescence) to blue (high fluorescence) to allow the simultaneous investigation of an additional cellular parameter. The movie shows that in the presence of 2 μM BDM, although the calcium signal is elevated in a stable manner and ICAM-1–GFP accumulates at the T cell–B cell interface, this interface is narrow (as most easily seen by the tightly concentrated ICAM-1–GFP accumulation) and no bead movement is seen. The movie compresses 20 min of experiment into 1 min of movie.
39. Three categories of bead movement were observed. Movement toward the interface was defined as bead movement at least one-fourth of a T cell circumference toward the interface (as shown in Fig. 1). Movement away from the interface was defined as bead movement at least one-fourth of a T cell circumference away from the interface, indicative of random bead movement. Beads located at the interface at the moment of T cell activation constituted <25% of all beads bound to T cells, consistent with the observation that migrating T cells move the beads toward their posterior. The only exception occurs after treatment with the PI 3-kinase inhibitor wortmannin, when 75% of the beads are already at the interface at the time of T cell activation, indicative of a lack of polarization. In this case, the beads are likely to initiate the cell-cell interaction by binding to ICAM-1 on both cells simultaneously. Beads that started at the interface stay there without exception. Beads that are scored "no movement" are those that move less than one-fourth of a T cell circumference in at least 5 min (Fig. 2).
40. Blocking antibodies were used at 10 μg/ml. We used YN1 as anti–ICAM-1 (*31*), 16-10A1 (Pharmingen) as anti–B7-1, GL1 (Pharmingen) as anti–B7-2, HM48-1 (Pharmingen) as anti-CD48, 37.51 (Pharmingen) as anti-CD28, and MK2.7 as anti-VCAM (*33*). Wortmannin was used at 100 nM, Ni^{2+} at 5 mM, and both were added directly to the microscopy dish. T cells were preloaded with BAPTA in parallel with Fura-2 at 20 μM. The ICAM-1–GFP construct has been described (*9*); the B7-2–GFP construct is strictly analogous, with the GFP attached to the cytoplasmic tail. Stable transfectants were selected for GFP expression using flow cytometry, and single cells were cloned.
41. Lack of T cell polarization is indicated by the fact that few activated cells had beads at the interface, by the lack of uropods and extended lamellipodia, and by the failure to migrate (*16*).
42. BDM (Sigma) was added to the T cells at the indicated concentrations 5 min before the start of the microscopy experiment from a fresh 200 μM stock in PBS. Noxius toxin (Alomone Labs, Jerusalem, Israel) was added to the T cells at 100 nM, that is, a 100-fold excess over the apparent dissociation concentration of blocking peak potassium channels 5 min before the start of the microscopy experiment.
43. The results were derived from a composite analysis of at least five experiments (nine on average) performed on at least three different days for each condition. As discussed in (*34*), composite data sets are shown because of the small number of cells per experiment that could be analyzed for some parameters. Positive controls were run on each day of the experiments to ensure uniformity.

44. We thank M. D. Sjaastad, W. J. Nelson, R. S. Lewis, and D. A. Lauffenberger for helpful discussions. Supported by the Howard Hughes Medical Institute and the European Molecular Biology Organization (C.W.).

31 August 1998; accepted 10 November 1998